



# Exogenous 6-benzylaminopurine inhibits tip growth and cytokinesis via regulating actin dynamics in the moss *Physcomitrium patens*

Jingtong Ruan<sup>1</sup> · Peishan Yi<sup>1</sup>

Received: 3 March 2022 / Accepted: 8 May 2022

© The Author(s), under exclusive licence to Springer-Verlag GmbH Germany, part of Springer Nature 2022

## Abstract

**Main conclusion** Exogenous BAP but not 2iP disrupts actin structures and induces tip-growth retardation and cytokinesis failure in the moss *Physcomitrium patens*.

**Abstract** Synthetic cytokinins have been widely used to address hormonal responses during plant development. However, exogenous cytokinins can cause a variety of cellular effects. A detailed characterization of such effects has not been well studied. Here, using *Physcomitrium patens* as a model, we show that the aromatic cytokinin 6-benzylaminopurine (BAP) inhibits tip growth at concentrations above 0.2  $\mu\text{M}$ . At higher concentrations (0.6–1  $\mu\text{M}$ ), BAP can additionally block mitotic entry and induce cytokinesis defects and cell death. These effects are associated with altered actin dynamics and structures. By contrast, 2-isopentenyladenine (2iP) does not cause marked defects at various concentrations up to 10  $\mu\text{M}$ , while t-zeatin (tZ) can moderately inhibit moss growth. Our results provide mechanistic insight into the inhibitory effects of BAP on cell growth and cell division and call for attention to the use of synthetic cytokinins for bioassays.

**Keywords** Actin · 6-Benzylaminopurine · Cell division · Cell growth · Cytokinin · *Physcomitrium*

## Abbreviations

BAP 6-Benzylaminopurine  
2iP 2-Isopentenyladenine  
tZ T-Zeatin  
ROP Rho of plants

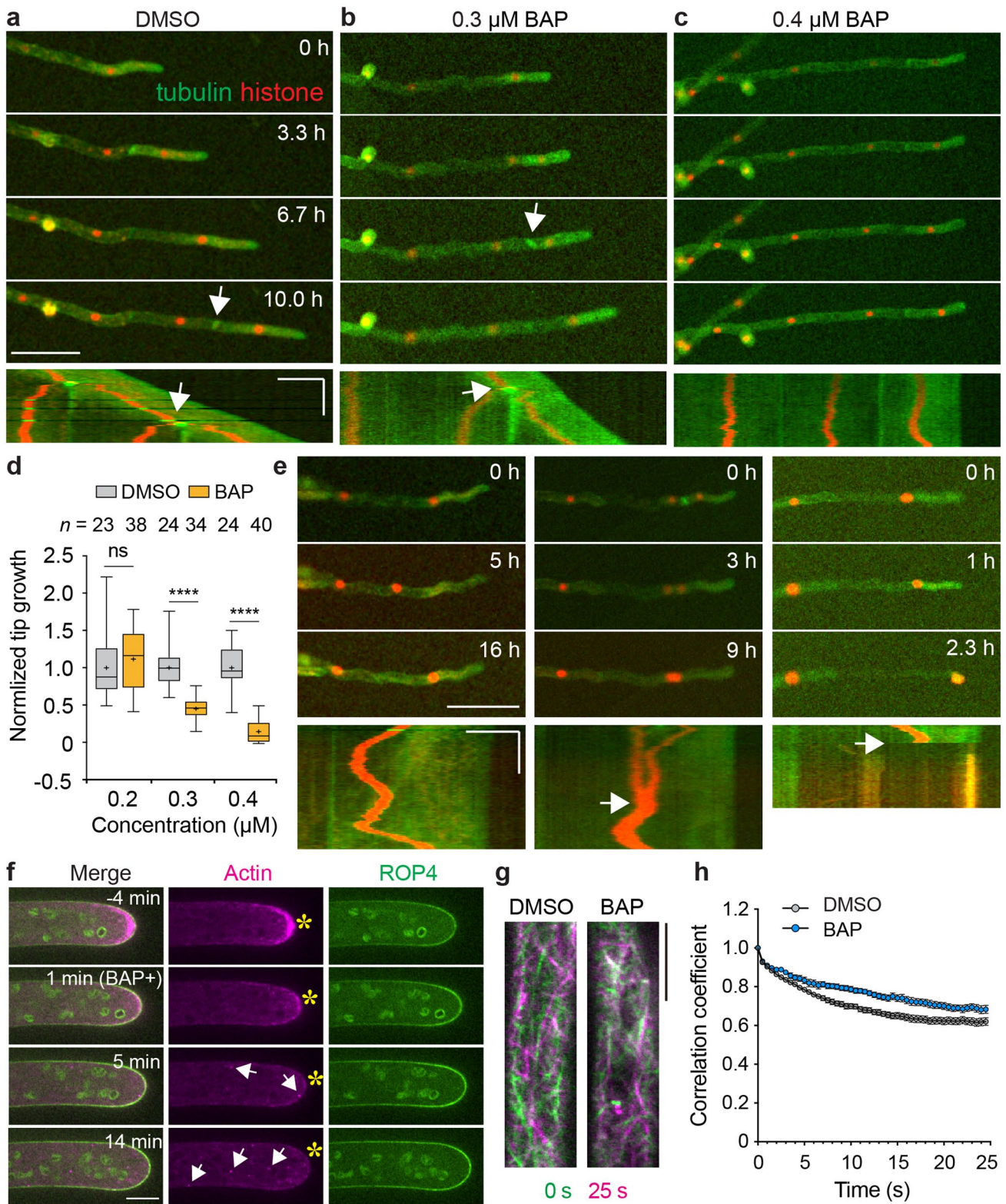
## Introduction

Cytokinins are phytohormones discovered for their ability to promote cell division and regulate plant development (Wybouw and De Rybel 2019). Shortly after its discovery, cytokinins are found to specifically induce gametophore bud formation in the moss *Tortella caespitosa* (Bert and Robert 1957). Since then, synthetic cytokinins such as 6-benzylaminopurine (BAP, also known as 6-benzyladenine or BA) have

been commonly used to study shoot development in mosses (Brandes and Kende 1968; Ashton et al. 1979). The effect of cytokinins varies depending on the concentration and chemical form (Szweykowska et al. 1969, 1971; Szweykowska and Korcz 1972). A low concentration of cytokinin promotes cell division, while a high concentration usually leads to reduced activity and retarded cell growth (Szweykowska et al. 1969, 1971; Szweykowska and Korcz 1972; Ashton et al. 1979; Thelander et al. 2005). The cytokinin signaling pathways have been extensively studied in seed plants and some of the key components are also characterized in mosses (Wybouw and De Rybel 2019; Guillory and Bonhomme 2021). However, how exogenous cytokinins affect cell growth and cell division remains poorly understood. In this study, we have carefully characterized the effects of exogenous BAP on cell growth and cell division in *P. patens*. We show that BAP could inhibit tip growth and cytokinesis by altering actin structures and dynamics, while 2-isopentenyladenine (2iP, also known as iP, IPA, or i<sup>6</sup>Ade) and t-zeatin (tZ) exhibit little and moderate effects on cell growth and moss development, respectively.

✉ Peishan Yi  
yipeishan@scu.edu.cn

<sup>1</sup> Key Laboratory of Bio-Resource and Eco-Environment of Ministry of Education, College of Life Sciences, Sichuan University, No. 24 South Section 1, Yihuan Road, Wuhou District, Chengdu, Sichuan 610065, People's Republic of China



## Materials and methods

### Strains and growth conditions

All strains used in this study originated from the Gransden ecotype of *Physcomitrium patens* (Ashton et al. 1979). Plants were routinely cultured at 25 °C on BCDAT plates under continuous light. For live-cell imaging, protonemata

**Fig. 1** Exogenous BAP inhibits tip growth in the moss *Physcomitrium patens*. **a–c** The tip growth of caulonema cells treated with DMSO (control) or BAP. Cells are labeled with GFP-tubulin (green) and H2B-RFP (red). The corresponding kymographs of each cell are shown below. Time is shown in hours (h). Arrows indicate cell division. Scale: image = 100  $\mu\text{m}$ ; Kymograph = 50  $\mu\text{m}$  (horizontal) and 5 h (vertical). **d** Quantification of the growth rate of tip cells. At each concentration, the growth rate of BAP-treated cells was normalized to a parallel control. Boxes with whiskers (min to max) show the interquartile range. Median and mean values are indicated by the crossline and “+,” respectively. The number of cells for quantification is shown above the plot. Statistical analyses are performed using unpaired *t* tests. ns, not significant; \*\*\*\*,  $P < 0.0001$ . **e** Nuclear migration (left), cytokinesis (middle), and cell death (right) in cells treated with 0.6  $\mu\text{M}$  BAP. Arrows indicate cytokinesis failure (middle) and cell death (right) in the above images. Scale: image = 100  $\mu\text{m}$ ; Kymograph = 50  $\mu\text{m}$  (horizontal) and 5 h (vertical). **f** The localization of actin (magenta) and ROP4 (green) in a tip cell treated with 1  $\mu\text{M}$  BAP. Time is shown in minutes (min). Stars indicate the apical membrane. Arrows show puncta-like structures. Note that actin accumulation at the tip was abolished, while the membrane localization of ROP4 was increased. Scale: 10  $\mu\text{m}$ . **g** Overlaid images of F-actin localization in the control (DMSO) and BAP-treated cells over time. Green, 0 s; magenta, 25 s. Scale: 10  $\mu\text{m}$ . **h** Quantification of time-course correlation coefficients for F-actin dynamics. Mean  $\pm$  SE; DMSO ( $n = 13$  cells); BAP ( $n = 11$  cells)

were inoculated on a thin layer of solid BCD medium in 6-well or 35-mm dishes and cultured for 5–7 days as described before (Miki et al. 2016; Yamada et al. 2016).

## Chemical treatment

For low-magnification imaging, the BCD medium surrounding the protonemata was carefully removed. Subsequently, 500  $\mu\text{L}$  of liquid BCD solution containing the desired concentration of DMSO (control), BAP, or 2iP was added directly to the plants. Imaging was performed immediately after chemical addition. For transient treatment, the BCD medium surrounding the protonemata was not removed. Instead, 200  $\mu\text{L}$  of liquid BCD medium containing DMSO or 1  $\mu\text{M}$  BAP/2iP was directly added to the plants. After keeping the samples at room temperature for five or ten minutes, the liquid solution was carefully removed and the imaging was performed. For high-resolution imaging, 1 mL of ddH<sub>2</sub>O was added to the plants and kept at room temperature for 30 min to equilibrate the medium. After that, the samples were imaged. When the cells developed to the desired stage, 200  $\mu\text{L}$  of liquid BCD medium containing DMSO or 1  $\mu\text{M}$  BAP was added to the plants. For FM4-64 staining, 100  $\mu\text{L}$  of ddH<sub>2</sub>O containing 5  $\mu\text{M}$  FM4-64 was added to the plants and kept in the dark for 30 min. After that, the FM4-64 solution was removed and the imaging was started. Colony growth assays were performed by inoculating small pieces of protonemata of similar sizes on BCDAT plates. After six days of culture, each colony was added with 50  $\mu\text{L}$  of ddH<sub>2</sub>O

containing 0, 1, 5, or 10  $\mu\text{M}$  t-zeatin or 2iP and cultured for another 12 days.

## Live-cell imaging

For low-magnification imaging, a Nikon TE2000-E microscope equipped with a 10 $\times$ 0.45-NA lens, a Zyla 4.2P CMOS camera (Andor), and a Nikon Intensilight Epi-fluorescence Illuminator was used. Images were taken at an interval of 10 min with in-between white light. For high-resolution imaging, the imaging system consisted of a Nikon Ti microscope, a CSU-X1 spinning disk confocal scanner unit (Yokogawa), an EMCCD camera (ImagEM, Hamamatsu), a 60 $\times$ 1.2-NA or 100 $\times$ 1.45-NA lens, and 561-nm and 488-nm laser lines (LDSYS-488/561-50-YHQSP3, Pneum). Images were taken at an interval of one or two minutes for monitoring tip growth and mitosis and at an interval of 0.5 s for imaging actin dynamics.

## Image processing and data analyses

All the images were processed and measured for quantification using the Fiji software (<https://imagej.net/software/fiji/>) (Schindelin et al. 2012). The correlation coefficient of actin localization was analyzed with the CorrelationJ 1o plugin in the fixed slide mode. The size of local region was set to three and the statistic to correlate was Average. Statistical analyses were performed using the unpaired Student's *t* test. The sample size ( $n$ ) has been indicated in the main text or figure legends where necessary.

## Results

### Exogenous BAP inhibits tip growth in a dose-dependent manner

To investigate the cellular effects of cytokinins in mosses, we focused on BAP, one of the most commonly used cytokinins. We performed long-term time-lapse imaging of protonema cells of a *P. patens* transgenic line under a low-magnification epi-fluorescence microscope following the previous protocol (Miki et al. 2016) with minor modifications (see “Materials and methods”). This transgenic line carries green fluorescent protein-tagged tubulin (GFP-tubulin) and red fluorescent protein-tagged histone (H2B-RFP) reporters, which label the entire cell and nucleus, respectively, and allow us to simultaneously visualize cell growth and cell division. As shown in Fig. 1a and Video S1, in the control experiments (DMSO treatment), caulonema tip cells could rapidly elongate and grew at a speed of 11–18  $\mu\text{m}/\text{h}$ . The growth rate was comparable to non-treated cells observed in our previous report (Yi and Goshima 2020). Therefore, under these conditions,

protonema development was not influenced. At 0.2  $\mu\text{M}$ , BAP did not affect tip growth and cell division (Fig. 1d). However, treatment with 0.3  $\mu\text{M}$  BAP significantly suppressed tip growth and reduced the growth rate to  $\sim 50\%$  of control cells (Fig. 1b, d, Video S2). At 0.4  $\mu\text{M}$ , tip growth was almost completely blocked (Fig. 1c, d, Video S3). When 0.6  $\mu\text{M}$  BAP was applied, additional phenotypes including irregular nuclear movement, cytokinesis failure, and abrupt cell death were observed (Fig. 1e, Videos S4–S6). At 1  $\mu\text{M}$ , 90% of the tip cells died within 6 h ( $n=31$ ). These data indicate that exogenous BAP can potently inhibit tip growth and cell division in a dose-dependent manner.

To further verify the inhibitory effects of BAP, we conducted a transient treatment experiment. Gel-supported protonema cells were treated with 200  $\mu\text{L}$  of 1  $\mu\text{M}$  BAP for five or ten min. As shown in Fig. S1a, tip cells were strongly inhibited immediately following treatment. 7–12 h later, the tip growth was largely resumed (Fig. S1c). Quantification analyses revealed prolonged inhibitory effects by 10-min treatment (Fig. S1d). In addition to tip cells, we also observed cytokinesis failure and the lack of a bulge during the division of subapical cells (Fig. S1b). In bulge-defective cells, the position of the nucleus and the division plane was displaced. This phenotype resembles the observation in the actin-depleted cells and *rop* mutants and supports our previous finding that bulge formation is essential for nuclear migration and asymmetric division (Yi and Goshima 2020). Hence, exogenous BAP inhibits polarized tip growth without cell specificity.

### BAP disrupts actin structures and influences actin dynamics

The Rho-of-plants (ROP) GTPases and actin filaments (F-actins) are master regulators of tip growth in mosses (Burkart et al. 2015; Cheng et al. 2020; Yi and Goshima 2020). To ask how BAP may inhibit tip growth, we examined the localization of endogenous ROP4 fused with an N-terminal mNeonGreen and actins visualized by a Lifeact-mCherry reporter (Yi and Goshima 2020). Before treatment, ROP4 and F-actins displayed polar localization on the apical membrane and in the cytoplasm, respectively (Cheng et al. 2020; Yi and Goshima 2020). When 1  $\mu\text{M}$  BAP was added, F-actin accumulation was immediately abolished (Fig. 1f, Video S7). Actins turned into puncta-like structures throughout the cytoplasm. This phenotype is highly reminiscent of that observed by Latrunculin B treatment (Vidali et al. 2009). Correlation analyses of residual cortical F-actins over time showed a reduced dynamicity (Fig. 1g, h, Videos S8–S9). Hence, BAP may disrupt actin structures by inhibiting actin polymerization and dynamics. In contrast, the membrane localization of ROP4 was not reduced but was enhanced. Concurrently, the apical membrane expanded

laterally and the tip growth was retarded (Fig. 1f, Video S7). A similar phenotype was also observed in subapical cells (Fig. S1e). In a previous report, N-terminal tagging was found to severely impact ROP function and this effect could be avoided using an internal tag (Cheng et al. 2020). However, our previous rescue experiments suggest that N-terminally tagged ROP4 is at least partially functional (Yi and Goshima 2020). More importantly, the N-terminally tagged ROP4 displays a similar localization pattern to the internally tagged version, though its membrane-labeled region is relatively expanded (Cheng et al. 2020; Yi and Goshima 2020). These facts suggest that N-terminal tagging could largely reveal the correct distribution of ROPs and the BAP-induced increase of ROP4 membrane localization should not be artifacts. Together, our results indicate that exogenous BAP attenuates tip growth via altering actin structures and dynamics but not disrupting ROP recruitment.

### 2iP has little or no effects on cell growth and moss development, while t-zeatin can moderately inhibit moss growth

To test whether the observed phenotypes can be induced by other cytokinins, we investigated the effects of 2iP with transient treatment. Surprisingly, under the same conditions, 1  $\mu\text{M}$  2iP did not cause any defects in tip growth or division (Fig. S1c and S1d). As the activity of cytokinin can be different depending on its chemical form (Szweykowska et al. 1969, 1971; Szweykowska and Korcz 1972; von Schwartzberg et al. 2007), we performed growth assays to assess whether a higher concentration of 2iP, as well as tZ, could impact cell growth and moss development. As shown in Fig. S2, 2iP exhibited little or no effects on colony growth at various concentrations up to 10  $\mu\text{M}$ . By contrast, tZ could moderately inhibit moss development. These results indicate that synthetic cytokinins BAP and tZ could inhibit cell growth to varying degrees, while the natural cytokinin 2iP does not at least at a concentration of 1–10  $\mu\text{M}$ . Such a difference is unlikely due to a lower sensitivity of 2iP to cytokinin receptors because 2iP can induce gametophore formation more efficiently than BAP and tZ in various moss species (Szweykowska et al. 1969, 1972; von Schwartzberg et al. 2007). Moreover, 2iP displays a higher binding affinity to moss cytokinin receptors than BAP and tZ (Lomin et al. 2021), which is different from that observed in *Arabidopsis* (Romanov et al. 2006). The different effects of 2iP, tZ, and BAP may also not result from the selective binding of distinct receptors because mutant analyses have demonstrated overlapping functions of the three canonical cytokinin receptors in *P. patens* in response to 2iP, tZ, and BAP (von Schwartzberg et al. 2016), although the involvement of other noncanonical receptors cannot be completely excluded (Gruhn et al. 2014). Alternatively, the metabolic

properties of 2iP, BAP, and tZ could play an important role. For example, iP-type cytokinins are efficiently secreted into the extracellular matrix and can be rapidly degraded by cytokinin oxidases, while both BA and tZ-type cytokinins are relatively stable and display a lower rate of export (Schulz et al. 2000; von Schwartzberg et al. 2007). Hence, BAP and tZ may produce prolonged effects in cells and contribute to the observed phenotypes. Most importantly, these results suggest that iP-type cytokinins are optimal for gametophore bud induction with minimal side effects in mosses.

### BAP induces cell cycle arrest and cytokinesis failure at a high concentration

Our results suggest that BAP could inhibit cell division when its concentration is  $> 0.4 \mu\text{M}$  (Fig. 1e, Video S5). To investigate the underlying cellular mechanism, we performed high-resolution time-lapse imaging in cells treated with  $1 \mu\text{M}$  BAP. Interestingly, the application of BAP before nuclear envelope breakdown (NEB) completely blocked mitotic entry. When BAP was added immediately after NEB, mitosis could proceed, but the cytokinesis failed. In these cells, the actin-marked phragmoplast and ROP4-labeled cell plate were not observed or could not extend to fuse with the parental membrane. Consequently, the daughter nuclei moved back to the cell center, which is a typical sign of cytokinesis failure (Fig. 2a, Videos S10–S11). To further visualize phragmoplast and cell plate assembly, we applied the lipophilic dye FM4-64 to the GFP-tubulin and H2B-RFP line. As shown in Fig. 2b, BAP did not block the formation of mitotic spindle and phragmoplast. The delivery of vesicles to the cell plate was also normal. However, the structure of phragmoplast could not be properly maintained and was disrupted in the central or peripheral regions, leading to fragmented cell plates (Fig. 2b, Video S12). Subsequently, the FM4-64 labeled membrane structures were degraded. To quantify how actin and MTs were affected, we compared the fluorescence intensity profile of Lifeact-mCherry and GFP-tubulin in normally dividing and cytokinesis-failed cells at the phragmoplast region when phragmoplast assembly was initiated. Surprisingly, no difference was observed in the intensity distribution of either actin or MT (Fig. 2c–e). However, among the four cytokinesis-failed cells, two did not form an actin-labeled phragmoplast (Fig. 2a) and the others assembled a phragmoplast that did not extend or fuse with the parental cell membrane. Instead, all cytokinesis-failed cells assembled MT-labeled phragmoplasts but could not maintain their structures (Fig. 2b). These results suggest that BAP inhibits cytokinesis by disrupting the assembly of actin structures on the phragmoplast and may not affect the actin pool and MT assembly. In support of this notion, a rapid loss of actin accumulation was also

observed in BAP-treated tip cells (Fig. 1f). Excess cytokinins have been well known to exhibit reduced activity in stimulating cell division (Szweykowska et al. 1971; Uzelac et al. 2012). In flowering plants, this phenomenon has been attributed to defects in the G1/S and G2/M transition of the cell cycle (Schaller et al. 2014). Our results indicate that a high concentration of BAP can additionally inhibit mitotic entry and cytokinesis, thus providing new insight into the mechanism of decreased cytokinin activity.

### Discussion

In conclusion, we have shown that exogenous BAP can potentially inhibit tip growth and cell division in the moss *P. patens*. The cellular defects are linked to altered actin dynamics and structures. Although non-specific cytotoxic effects of excess BAP may be in part responsible for the observed phenotypes, the dose-dependency also suggests potential interactions between cytokinins and actin during normal development. In mosses, gametophore buds are derived from side-branch initials which convert their growth from a tip-focused form to a diffusive pattern after cytokinin treatment (Bopp 1984). This phenomenon can be reversed by cytokinin removal (Brandes and Kende 1968). As tip growth largely depends on a focused actin network (Orr et al. 2020), it is likely that cytokinins negatively regulate actin assembly to promote the transition from tip growth to diffusive growth. However, with a strong effect, synthetic cytokinins such as BAP and tZ could lead to irreversible growth inhibition, cytokinesis failure, and even cell death. Such effects are not induced by natural cytokinins such as 2iP presumably due to their high turnover rate and mobility. Additionally, cytokinin-induced growth phenotypes can be suppressed through genetic manipulation (for example, in auxin-related mutants) (Ashton et al. 1979; Prigge et al. 2010), implying that the inhibitory effects caused by cytokinins are under genetic control. Moreover, cytokinin-induced gametophore formation is blocked in mutants of the ARPC1 subunit of actin nucleator ARP2/3 complex (Harries et al. 2005). Thus, cytokinin signaling can genetically interact with actin regulation in vivo. In flowering plants, cytokinins also alter actin organization during root cell elongation and defense response (Kushwah et al. 2011; Takatsuka et al. 2018; Pizarro et al. 2021). Hence, the regulation of actin by cytokinins might be conserved across the land plant lineage.

**Author contribution statement** PY conceived the project and wrote the manuscript. JR and PY performed the experiments and analyzed the data.

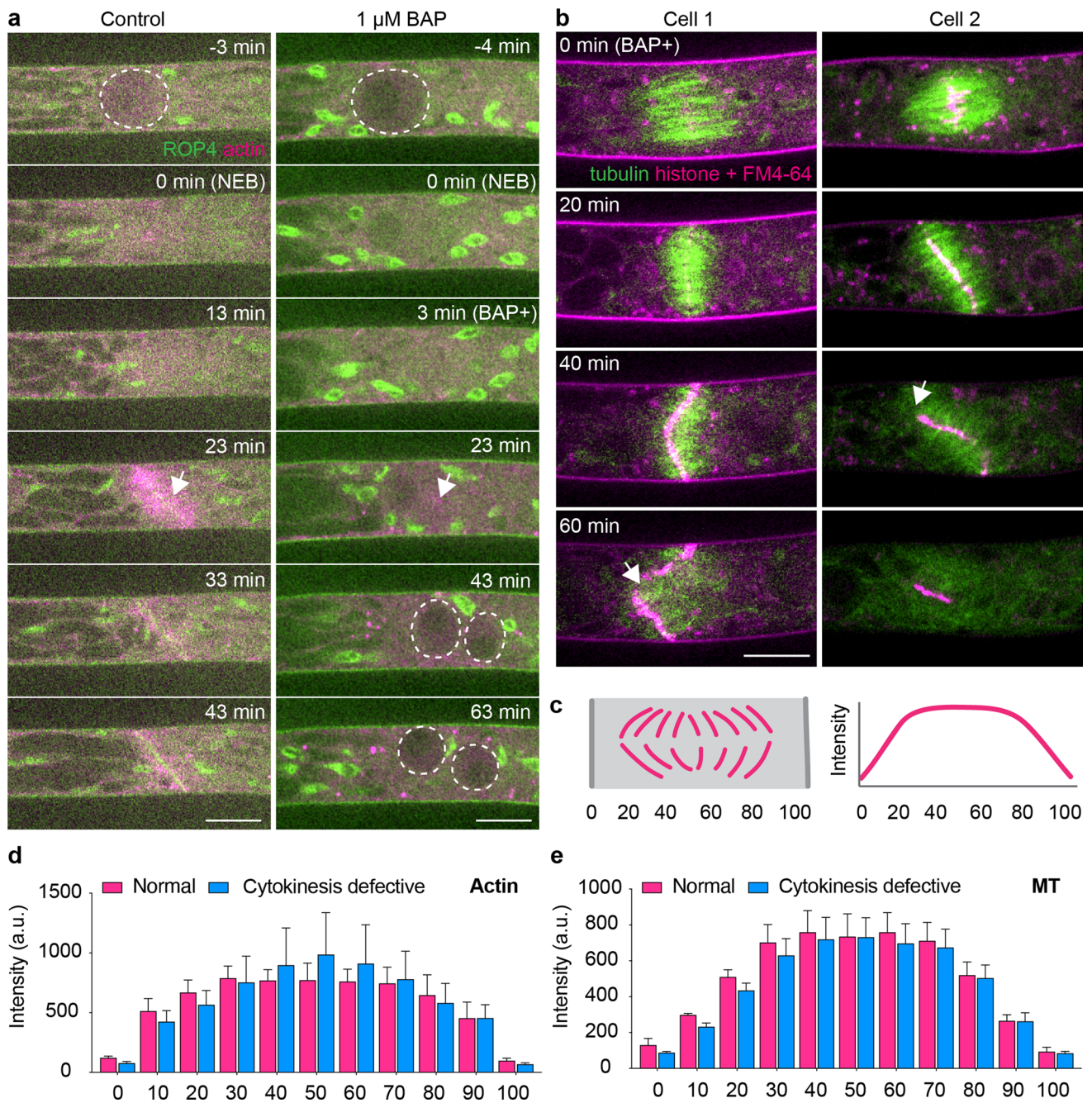


**Fig. 2** A high concentration of BAP causes cytokinetic defects. **a** Mitotic division of caulonema tip cells with (right) or without (left) BAP treatment. Cells are marked with mNeonGreen-ROP4 (green) and Lifeact-mCherry (magenta). The nucleus is indicated with dashed circles. Arrows show the position of a normal (left) or putative (right) cell plate in the control and BAP-treated cells, respectively. Note that ROP4 and actin localization is absent in BAP-treated cells. NEB, nuclear envelope breakdown. Time is shown in minutes (min). Scale: 10  $\mu$ m. **b** Phragmoplast assembly and vesicle delivery in dividing caulonema tip cells treated with 1  $\mu$ M BAP. Cells are marked with GFP-tubulin (green), H2B-RFP, and FM4-64 (magenta). Two representative cells are shown. Arrows indicate the corruption of

phragmoplast and cell plate at the middle (left) or peripheral (right) regions. Note that the FM4-64-labeled cell plate was eventually degraded after cytokinesis failure (right). Time is shown in minutes (min). Scale: 10  $\mu$ m. **c** Schematic illustration for the measurement of fluorescence intensity along the phragmoplast expanding direction. A rectangular region covering the entire initiated phragmoplast was drawn and the cell width was scaled to 100. Fluorescence intensity was plotted along the cell width. **d** Intensity plot of actin in normally ( $n=3$ ) dividing and cytokinesis-failed ( $n=4$ ) cells. **e** Intensity plot of MT in normally ( $n=3$ ) dividing and cytokinesis-failed ( $n=4$ ) cells. Mean  $\pm$  SE in **d** and **e**

**Supplementary Information** The online version contains supplementary material available at <https://doi.org/10.1007/s00425-022-03914-2>.

**Acknowledgements** This project is funded by a grant from the National Natural Science Foundation of China for Young Scientists (Grant no. 32100273) and an innovative research program (Grant no. 2022SCU0010) and a start-up grant (Grant no. 1082204112609) from Sichuan University to P.Y. Part of the work has been conducted in Gohta Goshima's lab at Nagoya University with the support from a long-term postdoctoral fellowship from the Human Frontier Science Program (LT000611/ 2018-L) to P.Y.

**Data availability** All data generated or analyzed during this study are included in this published article and its supplementary information files.

## References

- Ashton NW, Grimsley NH, Cove DJ (1979) Analysis of gametophytic development in the moss, *Physcomitrella patens*, using auxin and cytokinin resistant mutants. *Planta* 144(5):427–435. <https://doi.org/10.1007/BF00380118>
- Bert SG, Robert EE (1957) Development of the gametophyte in the moss *Tortella caespitosa*. *Bot Gaz* 119(1):31–38. <https://doi.org/10.1086/335957>
- Bopp M (1984) The hormonal regulation of protonema development in mosses: II. The first steps of cytokinin action. *Z Pflanzenphysiol* 113(5):435–444. [https://doi.org/10.1016/S0044-328X\(84\)80099-9](https://doi.org/10.1016/S0044-328X(84)80099-9)
- Brandes H, Kende H (1968) Studies on cytokinin-controlled bud formation in moss protonemata. *Plant Physiol* 43(5):827–837. <https://doi.org/10.1104/pp.43.5.827>
- Burkart GM, Baskin TI, Bezanilla M (2015) A family of ROP proteins that suppresses actin dynamics, and is essential for polarized growth and cell adhesion. *J Cell Sci* 128(14):2553–2564. <https://doi.org/10.1242/jcs.172445>
- Cheng X, Mwaura BW, Chang Stauffer SR, Bezanilla M (2020) A fully functional ROP fluorescent fusion protein reveals roles for this GTPase in subcellular and tissue-level patterning. *Plant Cell* 32(11):3436–3451. <https://doi.org/10.1105/tpc.20.00440>
- Gruhn N, Halawa M, Snel B, Seidl MF, Heyl A (2014) A subfamily of putative cytokinin receptors is revealed by an analysis of the evolution of the two-component signaling system of plants. *Plant Physiol* 165(1):227–237. <https://doi.org/10.1104/pp.113.2.28080>
- Guillory A, Bonhomme S (2021) Phytohormone biosynthesis and signaling pathways of mosses. *Plant Mol Biol* 107(4–5):245–277. <https://doi.org/10.1007/s11103-021-01172-6>
- Harries PA, Pan A, Quatrano RS (2005) Actin-related protein2/3 complex component ARPC1 is required for proper cell morphogenesis and polarized cell growth in *Physcomitrella patens*. *Plant Cell* 17(8):2327–2339. <https://doi.org/10.1105/tpc.105.033266>
- Kushwah S, Jones AM, Laxmi A (2011) Cytokinin-induced root growth involves actin filament reorganization. *Plant Signal Behav* 6(11):1848–1850. <https://doi.org/10.4161/psb.6.11.17641>
- Lomin SN, Savelieva EM, Arkhipov DV, Pashkovskiy PP, Myakushina YA, Heyl A, Romanov GA (2021) Cytokinin perception in ancient plants beyond angiospermae. *Int J Mol Sci* 22(23):13077. <https://doi.org/10.3390/ijms222313077>
- Miki T, Nakaoka Y, Goshima G (2016) Live cell microscopy-based RNAi screening in the moss *Physcomitrella patens*. *Methods Mol Biol* 1470:225–246. [https://doi.org/10.1007/978-1-4939-6337-9\\_18](https://doi.org/10.1007/978-1-4939-6337-9_18)
- Orr RG, Cheng X, Vidali L, Bezanilla M (2020) Orchestrating cell morphology from the inside out—using polarized cell expansion in plants as a model. *Curr Opin Cell Biol* 62:46–53. <https://doi.org/10.1016/j.ceb.2019.08.004>
- Pizarro L, Munoz D, Marash I, Gupta R, Anand G, Leibman-Markus M, Bar M (2021) Cytokinin modulates cellular trafficking and the cytoskeleton, enhancing defense responses. *Cells* 10(7):1634. <https://doi.org/10.3390/cells10071634>
- Prigge MJ, Lavy M, Ashton NW, Estelle M (2010) *Physcomitrella patens* auxin-resistant mutants affect conserved elements of an auxin-signaling pathway. *Curr Biol* 20(21):1907–1912. <https://doi.org/10.1016/j.cub.2010.08.050>
- Romanov GA, Lomin SN, Schmülling T (2006) Biochemical characteristics and ligand-binding properties of *Arabidopsis* cytokinin receptor AHK3 compared to CRE1/AHK4 as revealed by a direct binding assay. *J Exp Bot* 57(15):4051–4058. <https://doi.org/10.1093/jxb/erl179>
- Schaller GE, Street IH, Kieber JJ (2014) Cytokinin and the cell cycle. *Curr Opin Plant Biol* 21:7–15. <https://doi.org/10.1016/j.pbi.2014.05.015>
- Schindelin J, Arganda-Carreras I, Frise E, Kaynig V, Longair M, Pietzsch T, Preibisch S, Rueden C, Saalfeld S, Schmid B, Tinevez JY, White DJ, Hartenstein V, Eliceiri K, Tomancak P, Cardona A (2012) Fiji: an open-source platform for biological-image analysis. *Nat Methods* 9(7):676–682. <https://doi.org/10.1038/nmeth.2019>
- Schulz P, Reski R, Maldiney R, Laloue M, Kv S (2000) Kinetics of cytokinin production and bud formation in *Physcomitrella*: analysis of wild type, a developmental mutant and two of its *ipt* transgenics. *J Plant Physiol* 156(5–6):768–774. [https://doi.org/10.1016/S0176-1617\(00\)80246-1](https://doi.org/10.1016/S0176-1617(00)80246-1)
- Szweykowska A, Korcz I (1972) Inhibition of cell division in a moss protonema by some cytokinin isomers. *Planta* 108(3):279–282. <https://doi.org/10.1007/BF00384115>
- Szweykowska A, Schneider J, Prusińska U (1969) Studies on the specificity and sensitivity of the bud-induction response to cytokinins in the protonema of *Funaria hygrometrica*. *Acta Soc Bot Pol* 38(1):139–142. <https://doi.org/10.5586/ASBP.1969.014>
- Szweykowska AM, Dornowska E, Cybulska AM, Asiek GW (1971) The cell division response to cytokinins in isolated cell cultures of the protonema of *Funaria hygrometrica* and its comparison with the bud induction response. *Biochem Physiol Pflanz* 162:514–525. [https://doi.org/10.1016/S0015-3796\(17\)31185-X](https://doi.org/10.1016/S0015-3796(17)31185-X)
- Szweykowska A, Korcz J, Jaśkiewicz-Mroczkowska B, Metelska M (1972) The effect of various cytokinins and other factors on the protonemal cell divisions and the induction of gametophores in *Ceratodon purpureus*. *Acta Soc Bot Pol* 41:401–409. <https://doi.org/10.5586/aspb.1972.032>
- Takatsuka H, Higaki T, Umeda M (2018) Actin reorganization triggers rapid cell elongation in roots. *Plant Physiol* 178(3):1130–1141. <https://doi.org/10.1104/pp.18.00557>
- Thelander M, Olsson T, Ronne H (2005) Effect of the energy supply on filamentous growth and development in *Physcomitrella patens*. *J Exp Bot* 56(412):653–662. <https://doi.org/10.1093/jxb/eri040>
- Uzelac B, Janošević D, Stojičić D, Budimir S (2012) Effect of cytokinins on shoot apical meristem in *Nicotiana tabacum*. *Arch Biol Sci* 64(2):511–516. <https://doi.org/10.2298/ABS1202511U>
- Vidali L, Rounds CM, Hepler PK, Bezanilla M (2009) Lifeact-mEGFP reveals a dynamic apical F-actin network in tip growing plant cells. *PLoS ONE* 4(5):e5744. <https://doi.org/10.1371/journal.pone.0005744>
- von Schwartzberg K, Nunez MF, Blaschke H, Dobrev PI, Novak O, Motyka V, Strnad M (2007) Cytokinin in the bryophyte *Physcomitrella patens*: analyses of activity, distribution, and cytokinin oxidase/dehydrogenase overexpression reveal the role of extracellular cytokinins. *Plant Physiol* 145(3):786–800. <https://doi.org/10.1104/pp.107.103176>
- von Schwartzberg K, Lindner AC, Gruhn N, Simura J, Novak O, Strnad M, Gonneau M, Nogue F, Heyl A (2016) CHASE

- domain-containing receptors play an essential role in the cytokinin response of the moss *Physcomitrella patens*. *J Exp Bot* 67(3):667–679. <https://doi.org/10.1093/jxb/erv479>
- Wybouw B, De Rybel B (2019) Cytokinin—a developing story. *Trends Plant Sci* 24(2):177–185. <https://doi.org/10.1016/j.tplants.2018.10.012>
- Yamada M, Miki T, Goshima G (2016) Imaging mitosis in the moss *Physcomitrella patens*. *Methods Mol Biol* 1413:263–282. [https://doi.org/10.1007/978-1-4939-3542-0\\_17](https://doi.org/10.1007/978-1-4939-3542-0_17)
- Yi P, Goshima G (2020) Rho of plants GTPases and cytoskeletal elements control nuclear positioning and asymmetric cell division during *Physcomitrella patens* branching. *Curr Biol* 30(14):2860–2868. <https://doi.org/10.1016/j.cub.2020.05.022>

**Publisher's Note** Springer Nature remains neutral with regard to jurisdictional claims in published maps and institutional affiliations.

## Supplemental Information

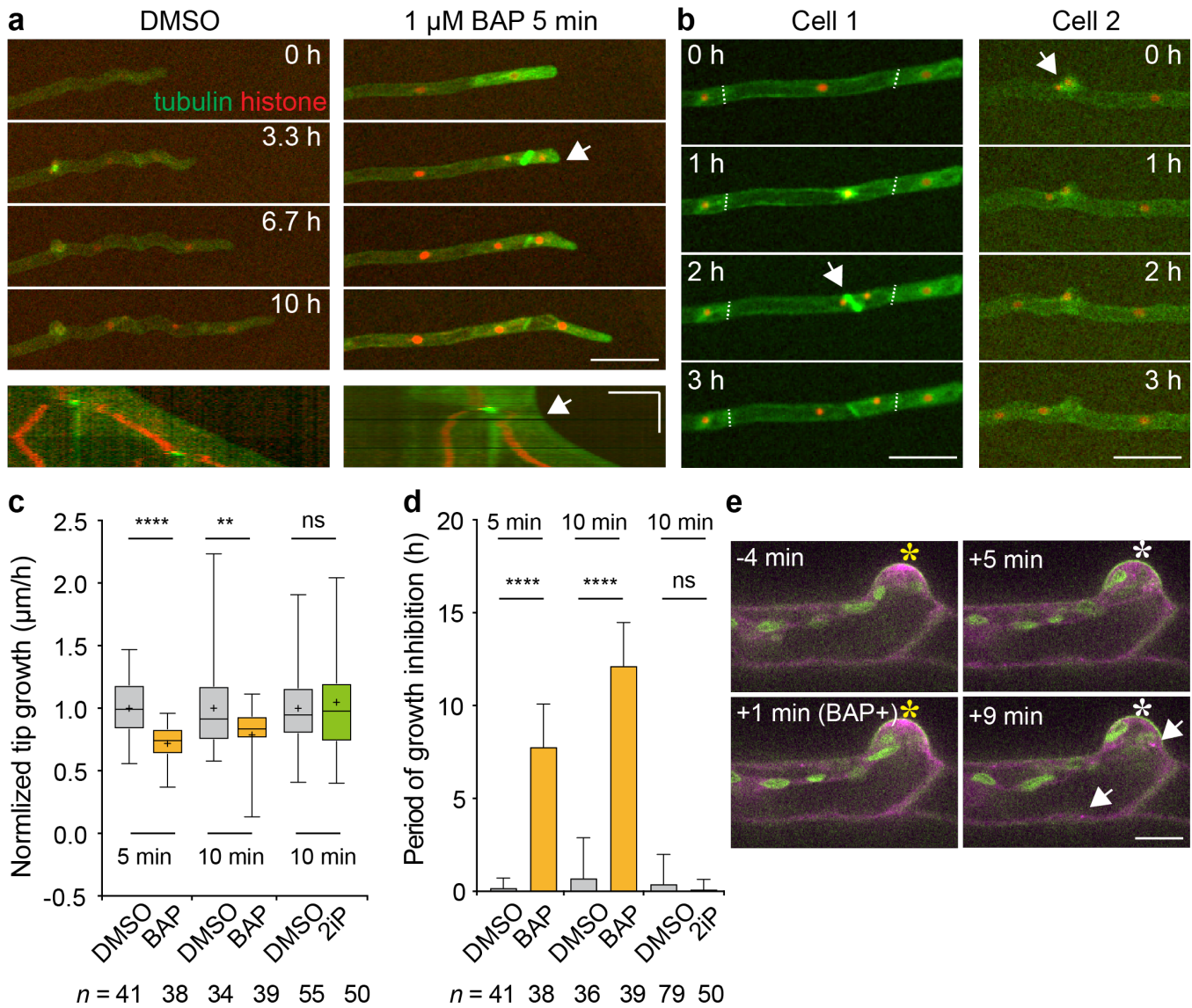


**Fig. S1** Transient treatment with BAP but not 2iP induces growth and division defects. **a** Tip growth in cells treated with 1  $\mu$ M BAP or DMSO (control) for five minutes. The corresponding kymograph of each cell is shown below. Arrows indicate the recovery of tip growth. Time is shown in hours (h). Scale: image, 100  $\mu$ m; Kymograph, 50  $\mu$ m (horizontal) and 5 h (vertical). **b** Defects in division plane positioning (left) and cytokinesis (right) in BAP-treated subapical cells. Arrows indicate the position of the division plane. Scale: 100  $\mu$ m. **c** Quantification of the growth rate of resumed tip-growing cells after transient treatment with DMSO (control) or 1  $\mu$ M BAP/2iP for five or ten minutes. The growth rate was normalized to control

cells. Boxes with whiskers (min to max) show the interquartile range. Median and mean values are indicated by the crossline and “+,” respectively. The number of cells for quantification is shown below the plot. Statistical analyses are performed using unpaired t-tests. ns, not significant; \*\*,  $P < 0.01$ ; \*\*\*\*,  $P < 0.0001$ . **d** Quantification of time displaying retarded growth in cells transiently treated with DMSO (control) or 1  $\mu\text{M}$  BAP/2iP for five or ten minutes. Mean  $\pm$  SE. Data analyses were the same as in **c**. **e** The localization of ROP4 (green) and actin (magenta) during bulge formation in subapical cells. Time is shown in minutes (min). Stars indicate the apical membrane. Arrows show puncta-like structures. Note that actin accumulation at the tip (yellow stars) was abolished (white stars). Scale: 10  $\mu\text{m}$ .

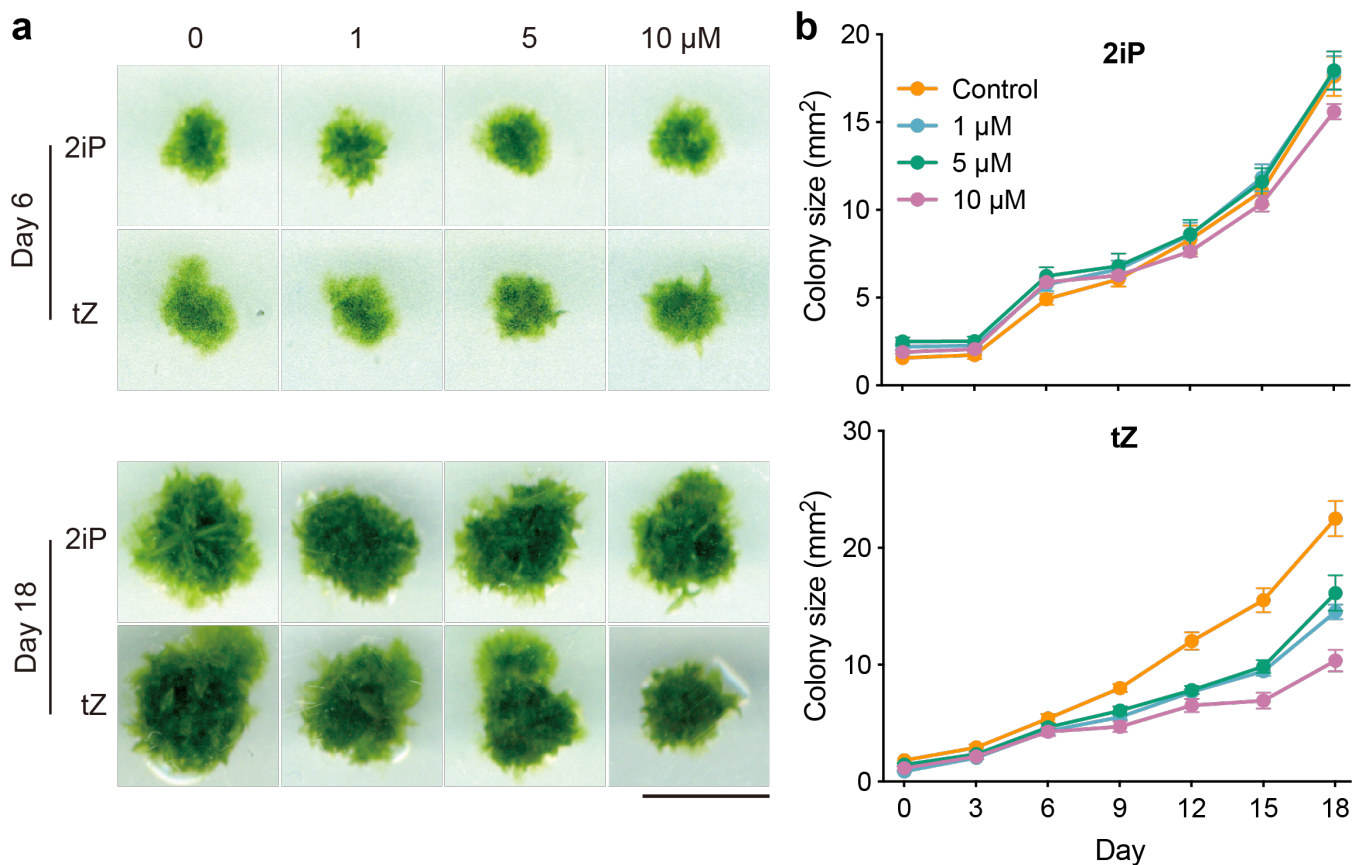


**Fig. S2** Effects of 2iP and tZ on colony growth. **a** Moss colonies grown on BCDAT plates. 2iP or tZ at various concentrations was added to each colony at day 6. Colonies were imaged every three days until day 18. Scale: 5 mm. **b** Quantification of 2iP-treated (above) and tZ-treated (below) moss colony size. Six

colonies were used for quantification in each group. Mean  $\pm$  SE. Note that 2iP did not induce marked defects in moss growth, while moss development was moderately inhibited by tZ.

**Video S1.** Tip growth of caulonema cells treated with DMSO. Cells are marked with GFP-tubulin (green) and H2B-RFP (red). The imaging interval is 10 minutes. The video is displayed at 15 fps. Strains and imaging conditions are the same in Video S2-S6.

**Video S2.** Partially suppressed tip growth of caulonema cells treated with 0.3  $\mu$ M BAP.

**Video S3.** Completely suppressed tip growth of caulonema cells treated with 0.4  $\mu$ M BAP.

**Video S4.** Irregular nuclear movement in a caulonema cell treated with 0.6  $\mu$ M BAP.

**Video S5.** Cytokinesis failure of a caulonema cell treated with 0.6  $\mu$ M BAP.

**Video S6.** Abrupt death of a caulonema cell treated with 0.6  $\mu$ M BAP.

**Video S7.** The localization of actin (magenta) and ROP4 (green) in a caulonema tip cell treated with 1  $\mu$ M BAP. BAP was added after the eighth frame. The imaging interval is one minute. The video is displayed at 15 fps.

**Video S8.** Actin dynamics in a DMSO-treated cell. The imaging interval is 500 milliseconds. The video is displayed at 15 fps.

**Video S9.** Actin dynamics in a cell treated with 1  $\mu$ M BAP. The imaging interval is 500 milliseconds. The video is displayed at 15 fps.

**Video S10.** The localization of actin (magenta) and ROP4 (green) in a control caulonema tip cell during cell division. The imaging interval is one minute. The video is displayed at 15 fps.

**Video S11.** The localization of actin (magenta) and ROP4 (green) in a caulonema tip cell treated with 1  $\mu$ M BAP during cell division. The imaging interval is one minute. The video is displayed at 15 fps.

**Video S12.** Defects in phragmoplast and cell plate assembly in a caulonema tip cell treated with 1  $\mu$ M BAP. The cell is marked with GFP-tubulin (green), H2B-RFP, and FM4-64 (magenta). FM4-64 labels the plasma membrane, intracellular vesicles, and cell plate. The imaging interval is two minutes. The video is displayed at 15 fps.